

# A Study on the Stability of Tailings Pond Based on Plastic Displacement and Safety Factor

Yadong Li\*

Hebei Construction Engineering Quality Inspection Center Co., LTD., Xiongan 070001, China

\*Corresponding author: Yadong Li, 1202201004@student.stdu.edu.cn

**Copyright:** © 2026 Author(s). This is an open-access article distributed under the terms of the Creative Commons Attribution License (CC BY 4.0), permitting distribution and reproduction in any medium, provided the original work is cited.

**Abstract:** The displacement deformation of tailings ponds serves as important early warning indicators for its instability, and accurately identifying plastic displacement is crucial for establishing a safety early warning system for tailings ponds. This study proposes a method for identifying plastic displacement in tailings ponds, systematically analyzes the variation pattern of plastic displacement with applied loads, and establishes the relationship between plastic displacement and the safety factor. The results indicate that the dam body is in the elastic deformation stage during the initial loading period. As the load increases, it enters the plastic deformation stage, and upon reaching the breaking load, the plastic displacement increases sharply. The maximum plastic displacements are 55.986 mm, 49.009 mm, and 44.197 mm, occurring at the sliding arc of the dam body. Furthermore, the safety factor exhibits a nonlinear inverse relationship with plastic displacement: the lower the safety factor, the greater the plastic displacement. Particularly when the safety factor drops below 1, the plastic displacement increases dramatically, indicating imminent dam failure. Based on these findings, the study provides an early identification basis for the instability risk of tailings ponds and proposes a scheme for establishing an effective early warning system, which holds significant engineering application value.

**Keywords:** Safety factor; Plastic displacement; Model experiment; Stability

**Online publication:** May 28, 2026

## 1. Introduction

A tailings pond is a facility constructed by building a dam at a valley entrance or enclosing an area to store tailings or other industrial wastes. In 2008, an extraordinarily severe dam failure accident occurred in Shanxi Province, China, resulting in 277 deaths and 4 missing persons (2021) <sup>[1]</sup>. In 2019, the Brumadinho tailings pond in Minas Gerais, Brazil, failed after being decommissioned for three years, causing 270 deaths or missing persons. Therefore, safety monitoring and disaster early warning for tailings ponds are of critical importance (2020) <sup>[2]</sup>.

Displacement is the main content of safety monitoring for tailings ponds and the most direct indicator for identifying their safety status. As a core content of safety assessment for tailings ponds, displacement

monitoring directly reflects the operational status and potential risks of the tailing's ponds. Currently, research on displacement monitoring in tailings dams mainly focuses on two aspects: one is the methods for obtaining displacement monitoring data, such as drones (2020) and distributed scatterer interferometric synthetic aperture radar (DS-InSAR) (2023) <sup>[3,4]</sup>. The other is the prediction of dam displacement using mathematical algorithms, such as the CS-SVM model (2021), BP neural network (2019), and grey theory (2017) <sup>[5-7]</sup>. It can be seen that the current processing of monitoring data is primarily based on pure algorithmic prediction, with insufficient consideration of the physical mechanisms of tailings pond deformation and its influencing factors. In 2019, the tailings pond in Minas Gerais, Brazil et al. had a deformation rate of -47 mm/a before its failure, whereas the Baiyan tailings pond of the Wengfu Phosphate Mine (2017) recorded a maximum settlement displacement of -57.8 mm/a in 2014 and has remained in safe operation to date <sup>[4,7]</sup>. Therefore, it is difficult to assess the stability of a tailings pond solely based on monitoring the total displacement. The reason is that many factors affect the displacement of tailings ponds, such as changes in the spatial distribution of the phreatic line, dam construction, and sliding of the tailings pond can all cause variations in the dam's displacement. Yan et al. proposed an intelligent method for extracting tailings pond information from high-resolution satellite images, but its accuracy for displacement monitoring in tailings ponds is insufficient <sup>[8]</sup>. Du et al. developed a novel InSAR time-series approach to obtain ground displacement maps of tailings ponds and to identify settlement caused by dam construction. Xie et al. studied the consolidation settlement patterns in the tailings pond area near the Great Salt Lake in Utah, and the results showed that high-resolution surface displacement measurements using InSAR can significantly improve our understanding of tailings settlement processes <sup>[2,9]</sup>. These studies indicate that while displacement monitoring data can be used to identify the operational characteristics of tailings ponds, but assessing the stability of a tailings pond solely based on total displacement is inaccurate. In fact, the key to determining the safety of a tailings pond lies in plastic displacement, and the identification of plastic displacement is particularly important. Therefore, how to identify plastic displacement from monitored displacement data has become a critical scientific and technological issue for early identification of tailings dam disasters and safety assessment. However, existing research has not yet given sufficient attention to this.

In summary, this study aims to fill the gap in research on displacement of tailings ponds. By deeply analyzing the mechanisms underlying displacement in tailings ponds, this paper innovatively proposes a method for identifying plastic displacement of tailings ponds. Specifically, a numerical model of the tailings pond is established using the finite element method to determine the elastic displacement in this study. By separating the elastic displacement from the measured total displacement, the plastic displacement is successfully identified, and the relationship between plastic displacement and the safety factor is established. This process reveals the dynamic characteristics of tailings pond deformation, and plastic displacement can be used to more directly and accurately assess the stability of the tailings pond. Based on this, a monitoring-data-based early identification and warning system for tailings pond instability and disaster prevention is proposed, significantly improving the accuracy and timeliness of tailings pond stability monitoring.

## **2. Model loading experiment of tailings pond**

### **2.1. Experimental device**

The model experiment was conducted in a model tank, which serves as the primary site for constructing the tailings pond model and performing the experiment. The tank measures 3.5 m in length, 1.2 m in width, and

1.5 m in height. The main body of the experiment tank is made of transparent tempered glass, reinforced with angle steel, and the outline of the tailings pond is marked on the outside of the tempered glass.

The material used for constructing the tailings dam is fine tailings sand. Through particle size gradation experiments, the uniformity coefficient of the fine tailings sand was found to be 9.08, and the curvature coefficient was 1.57, indicating that the particle distribution is uniform and suitable for use as dam construction material in tailings dam model experiments. In accordance with the “Standard for Geotechnical Test Methods”, experiments were conducted on the fine tailings sand, and the basic physical parameters obtained are shown in **Table 1**.

**Table 1.** Physical and mechanical parameters of tailings pond construction materials

Area	Dam construction material	Natural density/ (kg/m <sup>3</sup> )	Cohesive force/ (kPa)	Internal friction angle/(°)	Coefficient of permeability/(m/s)
Initial dam	Gravel	2400	15.00	40.00	$2.00 \times 10^{-4}$
Accumulation dam	Tail fine sand	1680	1.20	33.77	$1.43 \times 10^{-6}$

## 2.2. Experimental plan

During the experiment, pore pressure gauges were embedded in the tailings dam, and water was added to maintain a constant water level on the deposition beach, while the dam body was allowed to reach a steady-state seepage field. When constructing the tailings dam, lime was placed in layers to facilitate observation of dam deformation and arc formation. Subsequently, stepwise loading was applied at designated locations and when the readings from the pore pressure gauges remained constant, it indicated that the deformation induced by the current loading increment had been completed. After each loading, the dam body was scanned using a three-dimensional laser scanner with millimeter-level accuracy. The data before and after scanning were imported into post-processing software for analysis. Specifically, using the matching function of the post-processing software, the scanned data of the dam before and after loading were registered, and the coordinates of the same points before and after the load were extracted to obtain the displacement data of the tailings dam. The lime placement and loading process are shown in **Figure 1**. This experiment was divided into three groups. The initial dam slopes both inside and outside the tailings dam were 1:1.5. The dams in the three groups were 1:1.5, 1:2, and 1:2.5, respectively. The experimental conditions are detailed in **Table 2**.



**Figure 1.** Schematic of lime layering and loading process.

**Table 2.** Experimental conditions of tailings pond model

Case	Slope ratio of the initial dam	Slope ratio of the Accumulation dam
Case1		1:1.5
Case2	1:1.5	1:2
Case3		1:2.5

### 2.3. Analysis of experimental results

According to the results of the three-dimensional laser scanning in the experiment, we found that the displacement near the toe of the tailings dam slope was small, and no sliding occurred in this area when the tailings dam failed. Therefore, a total of four observation points were set at intervals of 10 cm downward from the crest of the stacked dam. The location of the points is shown in **Figure 2**.

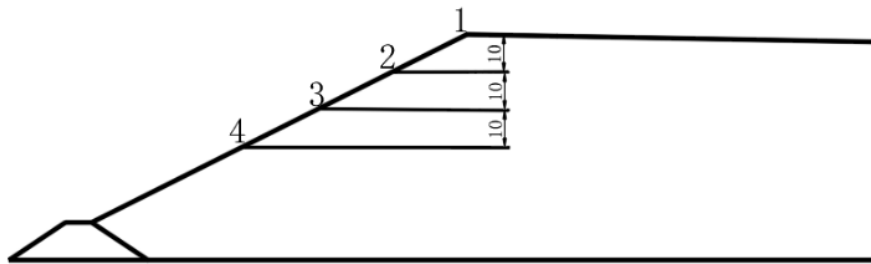


**Figure 2.** Schematic diagram of point selection.

Combining **Figure 3** and the experiment, it can be seen that after the first loading stage, the surface of the embankment dam showed almost no change, with only slight deformation. During the second loading stage, a slight depression appeared on the surface of the embankment dam, and settlement deformation began to occur in local areas. At this time, among the selected monitoring points, Points 1 and 2 exhibited slight displacement changes of approximately 4 mm. During the third loading stage, the displacement continued to increase, with a rising rate of increase. Entering the fourth stage, the dam body showed a tendency to slide downward, with displacements of points 1 and 2 increased to 20–22 mm and 18–19 mm, respectively, while the displacements of points 3 and 4 increased to 14–16 mm and 7–12 mm. By observing the displacement changes at the monitoring points, it is evident that points 1 and 2 experienced significantly greater increases in displacement, indicating significant damage tendencies in these areas, and the sliding failure of the dam gradually forms. In the final stage of loading, the displacements at various points of the dam increased sharply. In particular, the displacements at points 1, 2, and 3 reached 38–58 mm, and the displacement at point 4 reached 23–30 mm, indicating that these areas experienced severe deformation. The dam underwent a transition from local instability to overall failure, ultimately leading to the overall collapse of the tailings dam, as shown in **Figure 4**. A comparison of the three sets of experiments reveals that the larger the slope ratio of the accumulated dam, the smaller the load required for failure, while the displacement at failure becomes larger, and the sliding arc at failure becomes smaller. Specifically, when the accumulated dam slope ratio was 1:1.5, the failure load was 7.79 kPa, and the displacement at the maximum displacement monitoring point 2 at failure was 58 mm. When the slope ratio was reduced to 1:2 and 1:2.5, the failure load

increased to 11.69 kPa and 16.49 kPa, respectively, while the displacement at point 2 decreased to 51 mm and 46 mm. This is because a larger slope ratio raises the center of gravity of the dam and increases the slope angle, thereby increasing the sliding force and reducing the anti-sliding stability of the dam, which results in a smaller load required for failure. At the same time, as the slope ratio increases, stress concentration on the slope surface becomes more significant, leading to larger displacements at failure.

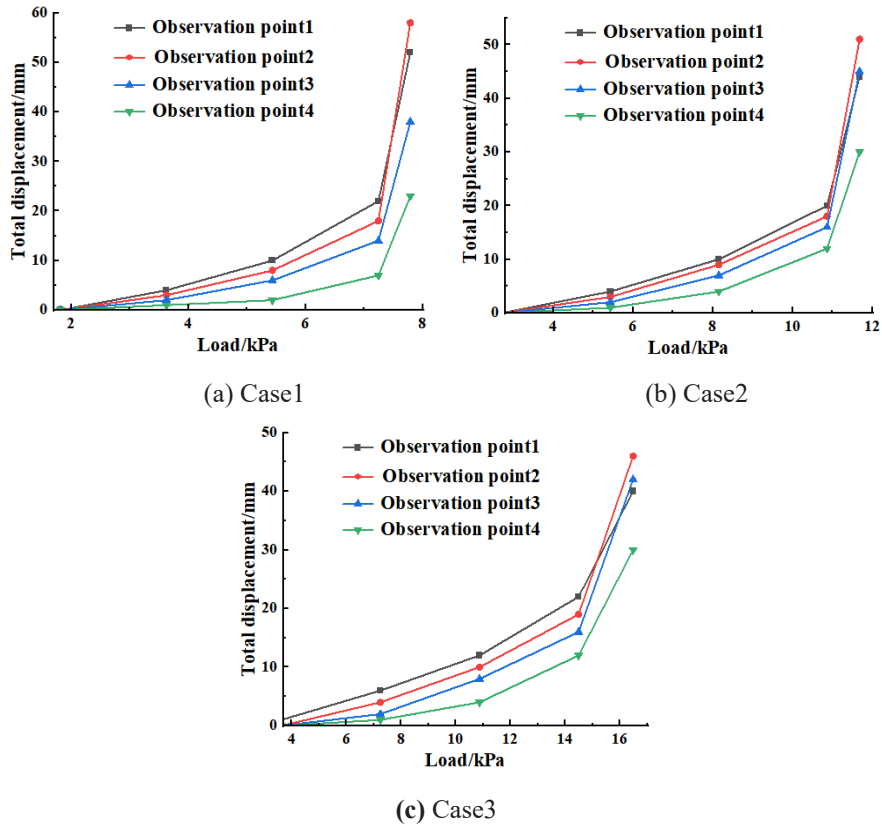


Figure 3. Load-Displacement relationship curve.



(a) Front view of tailings dam failure



(b) Side view of tailings dam failure

**Figure 4.** Tailings dam failure diagram.

### 3. Identification and analysis of plastic displacement

After completing the model experiments, the total displacement data of the tailings dam were obtained. To further analyze the plastic displacement of the tailings dam, a numerical simulation approach was adopted in this study. Using the ABAQUS finite element software, a numerical model of the tailings pond was established to simulate the displacement distribution of the tailings dam under different loading conditions. Based on the elastic-plastic displacement theory, the displacement before the occurrence of plastic strain is first identified as the elastic displacement, and then the elastic displacement is subtracted from the total displacement to obtain the plastic displacement. Meanwhile, the safety factors under corresponding working conditions were calculated through numerical simulation. The numerical simulation not only validated the experimental data but also further revealed the relationship between plastic displacement and the stability of the tailings dam, providing in-depth analysis and early warning basis for the instability of the tailings pond.

**Figure 5** shows the elastic displacements under different accumulated dam slope ratios. By locating the corresponding observation points in the figure, the elastic displacements at these points were obtained. Subsequently, the elastic displacements were subtracted from the total displacements measured in the experiments to obtain the plastic displacements at each point. For the different working conditions, the elastic displacements of observation points 1, 2, 3, and 4 were extracted. For the accumulated dam slope ratio of 1:1.5, the elastic displacements at the corresponding points were 2.622 mm, 2.014 mm, 1.423 mm, and 0.924 mm, respectively. For the slope ratio of 1:2, the elastic displacements were 3.239 mm, 1.991 mm, 1.237 mm, and 0.786 mm, respectively. For the slope ratio of 1:2.5, the elastic displacements were 2.936 mm, 1.803 mm, 0.965 mm, and 0.613 mm, respectively.

Based on the experimental data, the relationship curves between plastic displacement and uniformly distributed load are shown in **Figure 6**. It can be observed from **Figure 6** that during the first stage of loading, the dam body experienced slight deformation and remained within the elastic range. In the second stage of loading, the total displacement exceeded the elastic displacement, and the tailings dam entered the plastic deformation stage. Among the selected monitoring points, only points 1 and 2 reached a plastic displacement of 1 mm, indicating still relatively small displacements. In the third stage of loading, as loading continued, the plastic displacement further increased, and signs of sliding began to appear in the middle and upper parts of the dam body. In the fourth stage of loading, the maximum plastic displacements under

different working conditions increased to 19.38 mm, 16.76 mm, and 19.06 mm, respectively. By observing the displacement variations at these monitoring points, it is evident that Points 1 and 2 exhibited larger displacements, indicating that these have the most severe failure tendencies and could become the main weak points for sliding and instability of the tailings dam, with dam sliding failure gradually forming. In the final stage of loading, when the load reached the failure load, the tailings dam suddenly failed, and the plastic displacement increased sharply, with the maximum plastic displacement occurring at point 2. Using the laid lime, it was observed that the sliding arc and the most severely damaged area of the tailings dam were located around Point 2, where the surrounding region experienced significant plastic deformation. Compared with point 2, the plastic displacement at point 4 is smaller, which verifies the sliding characteristics of the dam failure, that is, sliding from the upper to the lower part, ultimately leading to the complete instability of the tailings dam.

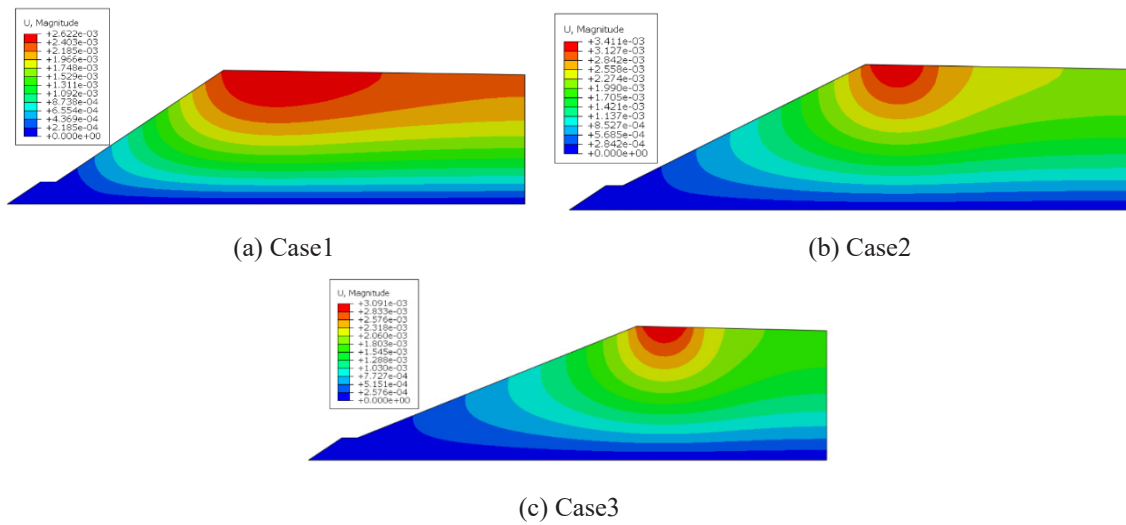
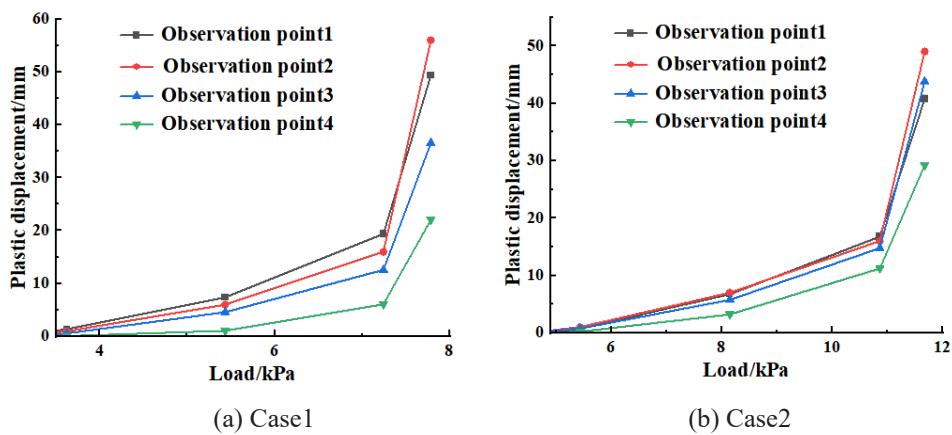
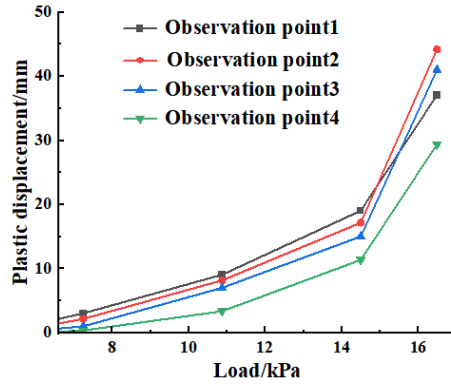


Figure 5. Elastic displacement diagram.





(c) Case3

Figure 6. Relationship between plastic displacement and load.

#### 4. Analysis of plastic displacement and safety factor

By selecting the maximum plastic displacement values under different load conditions for each working condition, and calculating the corresponding safety factors with finite element analysis, the relationship between plastic displacement and safety factor was established, as shown in **Figure 7**. It can be observed from **Figure 7** that the safety factor and plastic displacement exhibit an inverse relationship, and the variation is nonlinear. The safety factor decreases as the plastic displacement increases. When the safety factor is 1.458, the maximum plastic displacement is 1.378 mm. When the safety factor decreases to 1.179, 1.024, and 0.97, the plastic displacement increases to 7.378 mm, 19.378 mm, and 55.986 mm, respectively. Moreover, when the plastic displacement is small, the safety factor decreases rapidly. And when the plastic displacement is small, the safety factor decreases rapidly. As the safety factor approaches 1, the rate of decrease slows down, but the plastic displacement increases significantly. In particular, when the safety factor falls below 1, the plastic displacement increases sharply. The maximum plastic displacements under working conditions 1, 2, and 3 are 55.986 mm, 49.009 mm, and 44.197 mm, respectively, ultimately leading to the failure of the tailings dam. The tailings dam is mainly composed of fine tailings sand. Under external loads, the stress-strain relationship of the fine tailings sand exhibits significant nonlinear characteristics. Especially near the failure state, the strength of the material decreases, resulting in a rapid increase in plastic displacement. This nonlinear mechanical behavior is the fundamental reason why the safety factor decreases as plastic displacement increases. As the load continues to increase, the plastic deformation inside the tailings dam accumulates continuously, causing the shear strength of the material to gradually degrade. In the stage of small plastic displacement, the shear strength degrades relatively slowly, and the safety factor decreases rapidly; however, as plastic displacement further increases, the degradation of shear strength accelerates, the decreasing trend of the safety factor slows down, but the increase in plastic displacement becomes significantly larger. Particularly when the safety factor is close to or below 1, the strength of the tailings dam is approaching or has reached its limit state, and the plastic displacement increases dramatically, eventually triggering instability and failure of the dam body. This phenomenon indicates that the failure of the tailings dam often occurs when the safety factor is close to or below 1. At this stage, although the change in safety factor slows down, the deformation of the dam body intensifies significantly, ultimately leading to the instability and failure of the tailings dam. This analysis provides important theoretical support for the stability

assessment and design of tailings dams. An empirical formula can be fitted based on **Figure 7**.

$$y = 32.108x^{-8.35} \quad (1)$$

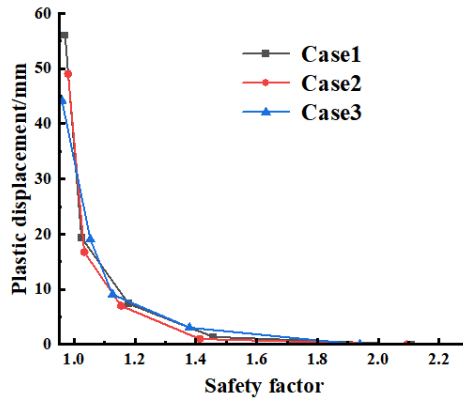


**Figure 7.** Relationship diagram between safety factor and plastic displacement.

## 5. Conclusion

Plastic displacement is a key factor affecting the stability of tailings ponds. This paper conducts an in-depth study on the plastic displacement of tailings ponds, using finite element software to establish a numerical calculation model. Through this model, the elastic displacement of the tailings pond is determined, and the plastic displacement is obtained in combination with experimental data. The relationship between plastic displacement and the safety factor is established, and an early identification and warning system for tailings pond instability disasters based on displacement monitoring data is constructed. The following conclusions are drawn:

- (1) In this study, model experiments of a tailings pond were conducted to simulate the deformation and failure process of the tailings dam under different loads, and the displacement data of the tailings dam under various loading conditions were obtained. This provides a reliable theoretical basis for understanding the deformation behavior of tailings ponds under different loads.
- (2) By establishing a finite element numerical calculation model, the elastic displacement of the tailings pond was determined, and the plastic displacement was calculated by combining it with the experimental data. It was found that at the initial stage of loading, the dam body is in the elastic deformation stage; as the load increases, the dam body enters plastic deformation, especially when the load reaches the failure load, the plastic displacement increases sharply. The maximum plastic displacements under different working conditions were 55.986 mm, 49.009 mm, and 44.197 mm, and these occurred at the sliding arc of the dam body.
- (3) The relationship between plastic displacement and the safety factor of tailings ponds was established, and it was found that the safety factor and plastic displacement exhibit an inverse nonlinear relationship. As the safety factor decreases, the plastic displacement increases significantly. In particular, when the safety factor falls below 1, the plastic displacement increases sharply, indicating that the dam body is approaching failure. Specifically, when the safety factor was 1.458, the maximum plastic displacement

was 1.378 mm; when the safety factor decreased to 0.97, the maximum displacement increased to 55.986 mm. Based on this, an early identification basis for the instability risk of the tailings pond can be provided, thereby enabling the establishment of an effective early warning system and the implementation of preventive measures in advance to ensure the safety of the tailings pond.

## Disclosure statement

The author declares no conflict of interest.

## References

- [1] Yao H, Cai L, Liu W, et al., 2021, Current Status and Development of Comprehensive Utilization of Waste Rock in Metal Mines in China. *The Chinese Journal of Nonferrous Metals*, 31(06): 1649–1660.
- [2] Du Z, Ge L, Ng A, et al., 2020, Risk Assessment for Tailings Dams in Brumadinho of Brazil Using InSAR Time Series Approach. *Science of the Total Environment*, 717: 137125.
- [3] Wang K, Yang P, Lv W, et al., 2020, Current Status and Development Trend of UAV Remote Sensing Applications in the Mining Industry. *Chinese Journal of Engineering*, 42(09): 1085–1095.
- [4] Wu H, Fan H, Zheng C, et al., 2023, Deformation Monitoring and Analysis of Tailings Dam Based on DS-InSAR: A Case Study of Brumadinho Mine in Brazil. *Metal Mine*, 2023(09): 169–176.
- [5] Hu J, Zhao Y, Luan C, et al., 2021, Deformation Prediction of Tailing Pond Dam Body Based on Cuckoo Search Optimized SVM. *Nonferrous Metals*, 11(09): 123–129.
- [6] Wang M, Wang B, Wang F, 2019, Tailings Dam Slope Stability Prediction Based on Genetic Algorithm-Optimized BP Neural Network. *Journal of Chifeng University*, 35(11): 113–115.
- [7] Zhen M, 2017, Application of Conventional Deformation Models in Monitoring Deformation of Tailings Dam and its Comparison. *Industrial Minerals & Processing*, 46(04): 38–40.
- [8] Yan D, Zhang H, Li G, et al., 2021, Improved Method to Detect the Tailings Ponds from Multispectral Remote Sensing Images Based on Faster R-CNN and Transfer Learning. *Remote Sensing*, 14(1): 103–103.
- [9] Xie H, Thomas O, Zhong L, et al., 2017, Consolidation Settlement of Salt Lake County Tailings Impoundment Revealed by Time-Series InSAR Observations from Multiple Radar Satellites. *Remote Sensing of Environment*, 202: 199–209.

### Publisher's note

Bio-Byword Scientific Publishing remains neutral with regard to jurisdictional claims in published maps and institutional affiliations.